Semiclassical fluid model of nonlinear plasmons in doped graphene

Bengt Eliasson[1,a)] and Chuan Sheng Liu[2,b)]
[1]SUPA, Physics Department, University of Strathclyde, John Anderson Building, Glasgow G4 0NG, Scotland, United Kingdom
[2]Departments of Physics and Astronomy, University of Maryland, College Park, Maryland 20742, USA

(Received 25 October 2017; accepted 19 December 2017; published online 4 January 2018)

A nonlinear fluid model of high-frequency plasmons in doped graphene is derived by taking fluid moments of the semi-classical kinetic equation for the electron gas. As a closure of the fluid moments, adiabatic compression is assumed with a given form of the distribution function, combined with an exact linear response based on the linearized Vlasov-Poisson system. In the linear regime, the model is in the long wavelength limit consistent with previous results using the random phase approximation for a two-dimensional electron gas, while it neglects the short-range interactions between massless Dirac fermions. The fluid model may be used to study the non-linear plasmonic wave mixing and optical coupling to lasers in graphene. https://doi.org/10.1063/1.5010402

I. INTRODUCTION

Graphene has unique electronic and material[1–5] properties, and plasmons in graphene is a field of intense research with important applications in optics, electronics, metamaterials, light harvesting, energy storage, THz technology, and so on.[6–8] Two-dimensional (2D) plasmons have been observed in monolayer graphite,[9] single layer graphene on SiC substrates,[10,11] epitaxial graphene,[12] etc. The linear dielectric response and properties of plasmons in graphene, initially treated in Refs. 13 and 14, are an active field of theoretical studies.[15–20] The wave frequency of low-energy 2D plasmons is typically proportional to the square root of the wavenumber, and observed 2D plasmons have wave-frequencies most commonly in the THz range or below. The properties of massless Dirac fermions also lead to that the frequency of 2D plasmons in graphene scales as the electron density raised to 1/4,[13,14] in contrast to that of Schrödinger electrons[21,22] where the frequency of 2D plasmons scales as the square root of the electron density. Nonlinear photonics have important applications in graphene with respect to harmonic generation and nonlinear electrodynamic response,[23–28] broadband optical limiting application,[29] four-wave mixing frequency conversion,[30–32] nonlinear generation of plasmons,[33] and other applications.[34–36] The self-interaction among large amplitude 2D plasmons leads to harmonic generation,[37] and their sidebands could be an important source of instability and localization of wave energy.[38–41] The aim of this paper is to develop a nonlinear fluid model of plasmons in graphene by using an adiabatic closure of the governing kinetic model. The model captures the main collective and statistical effects (e.g., the equation of state for the pressure) depending on the shape and evolution of the electron distribution function, as well as nonlinear effects leading to harmonic generation. Comparisons are made with fluid models of plasmons using a density of state closure of the fluid hierarchy,[42,43] with the linear dielectric response using random phase approximations,[13,14,21] and with the highly nonlinear response proposed for applications of harmonic generation.[23,24,37]

II. SEMI-CLASSICAL KINETIC MODEL

We here derive fluid-like equations for massless Dirac fermions starting from a semi-classical kinetic model. MKS (meter-kilogram-second) units are used throughout. While undoped graphene has the conduction band empty and the valence band filled at zero temperature, with no free carriers and a zero Fermi energy, doped or gated graphene has free carriers that support plasmons and screening of Coulomb interactions.[6,14] The latter is the subject of our study, where the free carriers consist of massless Dirac fermions. We adopt the semi-classical one-particle Hamiltonian $\mathcal{H} = v_F|\mathbf{p}| - e\phi(\mathbf{r},t)$ for massless Dirac fermions with constant speed v_F, where $v_F \approx 10^6$ m/s is the Fermi velocity, $\mathbf{p}$ is the momentum, ϕ is the potential, and $-e$ is the electron charge. It is one of the remarkable characteristics that the Fermi velocity is constant for massless Dirac fermions in graphene, in contrast to Schrödinger electrons where the Fermi velocity is density-dependent. Hamilton's equations

$$\frac{d\mathbf{p}}{dt} = -\frac{\partial \mathcal{H}}{\partial \mathbf{r}} = e\nabla\phi, \tag{1}$$

$$\frac{d\mathbf{r}}{dt} = \frac{\partial \mathcal{H}}{\partial \mathbf{p}} = v_F \frac{\mathbf{p}}{|\mathbf{p}|} \tag{2}$$

then lead to the collision-less one-particle Boltzmann (or Vlasov) equation

$$\frac{\partial f}{\partial t} + v_F \frac{\mathbf{p}}{|\mathbf{p}|}\cdot\nabla f + e\nabla\phi\cdot\frac{\partial f}{\partial \mathbf{p}} = 0. \tag{3}$$

The potential is given by[6]

$$\phi(\mathbf{r},t) = -\frac{e}{4\pi\epsilon_0\epsilon}\int \frac{(n_e(\mathbf{r}',t)-n_0)}{|\mathbf{r}-\mathbf{r}'|}d^2r', \tag{4}$$

a)bengt.eliasson@strath.ac.uk
b)chuanshengliu@gmail.com

where n_0 represents the areal number density of the neutralizing ion background, $n_e(\mathbf{r},t)=\int f\,d^2p$ is the electron areal number density, ϵ_0 is the electric vacuum permittivity, and ϵ is the mean dielectric constant of the surrounding medium.[6] The Vlasov equation (3) describes the evolution of the distribution function of massless Dirac fermions having velocity $\mathbf{v}=v_F\mathbf{p}/|\mathbf{p}|$ and constant speed $|\mathbf{v}|=v_F$ in the presence of the mean-field potential ϕ. This simplest kinetic model may be expanded by the inclusion of various nonideal effects.[44] Taking into account the quantum tunneling of the electrons at small scales, the Vlasov equation would be replaced by a Wigner equation for a pseudo-distribution function,[45,46] and taking into account spin effects where the single-particle wave-function is a 2-spinor would give rise to a 2×2 matrix of coupled kinetic equations[47,48] or an extension of the phase space to include the spin polarization variable.[49,50] For a fully degenerate 2D electron gas, it has, however, been found that by calculation of the gradient correction to the Fermi-Thomas model the quantum tunneling vanishes.[51,52] The present model takes into account the effect of low-dimensionality on the long-range Coulomb interactions[16] and the shape of the electron distribution function in momentum space of a two-dimensional electron gas (2DEG),[21] but neglects the short-range interactions between electrons that are important for plasmons in graphene at short wavelengths.[13,14] Linearizing and Fourier analyzing Eqs. (3) and (4) with $f=f_0+f_1$ and $\phi=\phi_1$, and f_1 and ϕ_1 proportional to $\exp(i\mathbf{q}\cdot\mathbf{r}-i\omega t)$, yields the dielectric function $\varepsilon_e=1+\chi_e$, where the electron susceptibility is given by

$$\chi_e=\frac{e^2}{2\epsilon_0\epsilon q}\int\frac{\mathbf{q}\cdot\nabla_p f_0}{(\omega-v_F\mathbf{p}\cdot\mathbf{q}/|\mathbf{p}|)}d^2p$$
$$=\frac{e^2v_F}{2\epsilon_0\epsilon q\omega^2}\int\frac{(\mathbf{q}\cdot\mathbf{p})^2-q^2|\mathbf{p}|^2}{|\mathbf{p}|^3[1-v_F\mathbf{p}\cdot\mathbf{q}/(|\mathbf{p}|\omega)]^2}f_0\,d^2p, \quad (5)$$

and the second step is obtained by an integration by parts. The equilibrium distribution function f_0 for the massless Dirac fermions can be taken to be a Fermi-Dirac momentum distribution function[23,24] $f_0=\alpha\{\exp[\beta(v_F|\mathbf{p}|-\mu)]+1\}^{-1}$ with $\beta=1/k_BT_e$ and α a normalization constant, which in the ultra-cold limit $\beta\mu\gg 1$ takes the form

$$f_0(\mathbf{p})=\frac{g_sg_v}{(2\pi\hbar)^2}H(-v_F|\mathbf{p}|+\mu)=\frac{n_0v_F^2}{\pi\mu^2}H(-v_F|\mathbf{p}|+\mu), \quad (6)$$

where $H(\xi)$ is the Heaviside function which equals one for $\xi>0$ and zero for $\xi<0$, $g_s=2$ and $g_v=2$ are the spin and valley degeneracies for graphene, $\mu=\hbar v_Fk_F$ is the chemical potential (the same as the Fermi energy in the ultra-cold limit), and $k_F=\sqrt{4\pi n_0/g_sg_v}$ is the Fermi wavenumber. The equilibrium distribution function f_0 is normalized such that $\int f_0\,d^2p=n_0$. The ultra-cold limit is assumed here for simplicity, but the obtained results can be extended to finite temperatures in a straightforward manner. Using the distribution function (6), the integral in Eq. (5) is evaluated to give

$$\chi_e=\frac{1}{\lambda_sq}\left(1-\frac{1}{\sqrt{1-v_F^2q^2/\omega^2}}\right), \quad (7)$$

with $q=|\mathbf{q}|$, and where $\lambda_s=\epsilon_0\epsilon\mu/(e^2n_0)$ is a screening length. The dispersion relation for plasmons, $1+\chi_e=0$, then gives

$$\omega^2=(v_Fq)^2\left(\frac{1}{\lambda_s^2q^2+2\lambda_sq}+1\right). \quad (8)$$

The dependence of the wave frequency on the wavenumber is plotted as a solid line in Fig. 1.

For small wavenumbers $\lambda_sq<1$, we have from Eq. (8) the approximate dispersion relation

$$\omega^2\approx(v_Fq)^2\left(\frac{1}{2\lambda_sq}+\frac{3}{4}\right)=\frac{e^2n_0q}{2\epsilon_0\epsilon m_*}+\nu v_F^2q^2. \quad (9)$$

In the last step, we denoted the density-dependent effective mass $m_*=\mu/v_F^2=\hbar k_F/v_F$, and for the comparisons of models below, a correction parameter $\nu=3/4$ is introduced. In experiment,[10] the measured density $n_0=1.9\times10^{14}\,\mathrm{m}^{-2}$ gives $k_F=\sqrt{\pi n_0}=0.077\,\text{Å}^{-1}$ and $m_*=0.089m_e$, in reasonable agreement with the obtained best-fit value $m_*=0.077m_e$. In Eq. (9), the first term on the right-hand side represents the space-charge effect, while the second term is due to the shape of the distribution function in momentum space. The typical square-root behavior of the frequency on wavenumber, keeping only the first term on the right-hand side of Eq. (9), is seen in the dashed curve in Fig. 1. The dispersion relation (9), plotted as a dash-dotted curve in Fig. 1, is on the same form as obtained by Stern[21] for a 2D electron gas using a random phase approximation. In the fluid model of Ref. 42 and subsequently used in Ref. 43, $\nu=1/2$ (instead of 3/4) was obtained using a density-of-states closure for the pressure. In graphene, it is predicted using a random phase approximation[13,14] that band overlap of the wavefunctions leads to a negative

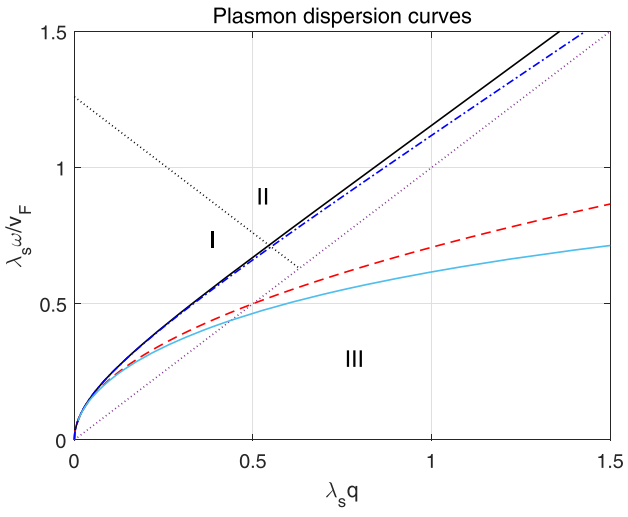

FIG. 1. Dispersion curves for plasmons in graphene obtained from kinetic theory (8) (solid black line), the approximate dispersion relation (9) (dash-dotted blue line), the RPA result (11) (solid magenta line), and the long-wavelength limit $\omega=v_F\sqrt{q/(2\lambda_s)}$ (dashed red line), for the case of graphene on a SiC substrate with $n_0=1.9\times10^{17}\,\mathrm{m}^{-2}$ and $\epsilon=5.5$, for which $k_F\lambda_s\approx0.63$. The dotted lines show the Fermi velocity cone $\omega=v_Fq$, and the boundary $\omega=2\mu/\hbar-v_Fq$ between the undamped region I and the Landau damped regions II and III due to interband and intraband transitions, respectively.

correction of the dispersion relation at large wavelengths. Starting from the electron susceptibility in the high-frequency ($\omega > v_F k$) long wavelength limit[14]

$$\chi_{e,RPA} = -\frac{q v_F^2}{2\lambda_s \omega^2}\left(1 - \frac{\omega^2}{4k_F^2 v_F^2}\right), \tag{10}$$

one obtains from the dispersion relation $1 + \chi_{e,RPA} = 0$ that

$$\omega^2 = \frac{(v_F q)^2}{2\lambda_s q + q^2/(4k_F^2)}. \tag{11}$$

As a comparison, the wave frequency obtained from Eq. (11) is plotted in Fig. 1 (solid magenta line), showing a frequency down-shift compared with the 2DEG case due to the short-range electron interactions in graphene. Keeping only the first correction for small q in Eq. (11) yields

$$\omega^2 = (v_F q)^2\left(\frac{1}{2\lambda_s q} - \frac{1}{16\lambda_s^2 k_F^2}\right) = \frac{e^2 n_0 q}{2\epsilon_0 \epsilon m_*} - \alpha_{ee}^2 v_F^2 q^2, \tag{12}$$

where $\alpha_{ee} = 1/(4\lambda_s k_F) = e^2/(4\pi\epsilon_0\epsilon\hbar v_F)$ is the fine structure constant;[6] hence, the correction parameter is negative, $\nu = -\alpha_{ee}^2$. Taking both the positive and negative corrections into account, Ref. 18 obtained $\nu = 3/4 - \alpha_{ee}^2$. It was pointed out in Ref. 18 that ν can be either positive or negative depending on the value of α_{ee}. For example, a suspended graphene sheet with $\epsilon = 1$ gives $\alpha_{ee} = 2.2$ and $\nu = -4.0$, while for graphene with one side exposed to air ($\epsilon_1 = 1$) and the other to SiC ($\epsilon_2 = 10$) giving $\epsilon = (\epsilon_1 + \epsilon_2)/2 = 5.5$ yields $\alpha_{ee} = 0.40$ and $\nu = 0.59$. The measured plasmon dispersion in Ref. 10 seems, however, to be consistent with the negative correction obtained in Refs. 13 and 14 at long wavelengths. Even though $\omega/q > v_F$ for all wavenumbers in our model (and hence no intraband transitions), it should be noted that Landau damping is predicted to take place due to interband transitions[13,14,18] in the region $\omega > v_F q$, $\omega > 2\mu/\hbar - v_F q = 2v_F k_F - v_F q$. This restricts the validity of our semiclassical model at large wavenumbers. As an example, interband transitions take place in region II in Fig. 1 for the case of graphene on a SiC substrate[10] with $\epsilon = 5.5$ and $n_0 = 1.9 \times 10^{17}\,\mathrm{m}^{-2}$. The dispersive and dissipative effects due to nonlinearity[27] are more complex, but may include interband transitions due to harmonic generation, etc.

III. NON-LINEAR FLUID MODEL DERIVED FROM KINETIC THEORY WITH ADIABATIC CLOSURE

Next, nonlinear fluid equations are derived using moments of the Vlasov equation. Integrating Eq. (3) over momentum space gives the continuity equation

$$\frac{\partial n_e}{\partial t} + \nabla\cdot(n_e \mathbf{v}_e) = 0, \tag{13}$$

where the fluid density n_e and velocity field $\mathbf{v}_e$ are defined as

$$n_e = \int f\, d^2p \tag{14}$$

and

$$\mathbf{v}_e = \frac{1}{n_e}\int v_F \frac{\mathbf{p}}{|\mathbf{p}|} f\, d^2p, \tag{15}$$

respectively. The fluid density n_e enters into Eq. (4) for the scalar potential. To obtain an equation for the fluid velocity, the Vlasov equation is multiplied by $\mathbf{p}$ and integrated over momentum space

$$\frac{\partial(n_e \mathbf{p}_e)}{\partial t} + v_F \nabla\cdot\int \frac{\mathbf{pp}}{|\mathbf{p}|} f\, d^2p - e n_e \nabla\phi = 0, \tag{16}$$

where the fluid momentum is defined as

$$\mathbf{p}_e = \frac{1}{n_e}\int \mathbf{p} f\, d^2p, \tag{17}$$

and $\mathbf{pp}$ denotes a dyadic product. The second term in the left-hand side of Eq. (16) represents the momentum flux due to the mean flow and statistical motion of the electrons. Equation (15) will be used below to connect $\mathbf{v}_e$ to $\mathbf{p}_e$ and n_e. Higher moments of the Vlasov equation can be found by multiplying Eq. (3) by $\mathbf{pp}$ and integrating over momentum space, and so on, leading to a hierarchy of fluid equations.

Here, a closure of the fluid hierarchy is found by assuming f to be on a specific form that approximately solves the Vlasov equation (3). Since the Vlasov equation describes an incompressible flow in phase space, the key idea is that the phase fluid density (the distribution function f) does not change in amplitude but only in width and offset in momentum space. Since the phase speed of the plasmon is larger than the Fermi velocity, the electrons are not able to stream to neutralize the wave potential. Similar to a three-dimensional electron gas,[53] the high-frequency plasmons thus lead to a deformation of the Fermi surface. We use a shifted Fermi-Dirac distribution function[54] to model adiabatic compression, keeping the chemical potential constant. Temporarily choosing a coordinate system such that the spatial variation is along the x-axis, the distribution function is assumed to be of the form

$$f(x,\mathbf{p},t) = \frac{n_0 v_F^2}{\pi\mu^2} H\left[-v_F\sqrt{\frac{(p_x - p_{ex})^2}{n_e^2/n_0^2} + p_y^2} + \mu\right], \tag{18}$$

where $p_{ex}(x,t)$ represents a shift of the mean momentum, and the density variations $n_e(x,t)$ are achieved by a widening and contractions of the distribution function along the p_x component in momentum space. The particular form of Eq. (18) ensures that Eqs. (14) and (17) are fulfilled exactly. Equation (15) is used to derive a nonlinear relation between $\mathbf{v}_e$, $\mathbf{p}_e$ and n_e, where $p_{ey} = 0$ and $v_{ey} = 0$ due to symmetry. Using that $\mathbf{p}/|\mathbf{p}| = \nabla_p|\mathbf{p}|$, the x-component of the right-hand side of Eq. (15) is readily integrated over p_x, with the result

$$n_e v_{ex} = 2\frac{n_0 v_F^3}{\pi\mu^2}\int_0^{\mu/v_F}\left(\sqrt{p_{x+}^2 + p_y^2} - \sqrt{p_{x-}^2 + p_y^2}\right) dp_y, \tag{19}$$

where $p_{x\pm} = p_{ex} \pm (n_e/n_0)\sqrt{\mu^2/v_F^2 - p_y^2}$. Equation (19) relates the fluid velocity v_{ex} nonlinearly to the fluid momentum p_{ex}

and density n_e, and when multiplied with the electron charge gives the x-component of the electric current density, $j_x = -en_e v_{ex}$. The nonlinear dependence of the current density on momentum has been proposed for the generation of odd harmonic in the case of a monochromatic electromagnetic driving field.[23,24] It should be noted that Eq. (19) can be written on a similar form as Eq. (6) of Ref. 23: Using the identity $\sqrt{p_{x+}^2 + p_y^2} - \sqrt{p_{x-}^2 + p_y^2} = (p_{x+}^2 - p_{x-}^2) \Big/ \left(\sqrt{p_{x+}^2 + p_y^2} + \sqrt{p_{x-}^2 + p_y^2}\right)$ and a change of integration variable $p_y = (\mu/v_F)\sin\varphi$, $dp_y = (\mu/v_F)\cos\varphi\, d\varphi$ in Eq. (19) gives, after some straightforward manipulations

$$n_e v_{ex} = n_e v_F \frac{4}{\pi} \frac{2P_F}{\sqrt{1+P_F^2}} \int_0^{\pi/2} \frac{\cos^2\varphi\, d\varphi}{(S_+ + S_-)}, \tag{20}$$

where

$$S_\pm = \sqrt{1 \pm 2\frac{n_e}{n_0}\frac{P_F\cos\varphi}{1+P_F^2} + \left(\frac{n_e^2}{n_0^2} - 1\right)\frac{\cos^2\varphi}{1+P_F^2}}. \tag{21}$$

Here, $P_F = v_F p_{ex}/\mu = p_{ex}/p_F$ is the dimensionless fluid momentum (equal to minus the field parameter Q_F in Ref. 23) and $p_F = \mu/v_F$ the Fermi momentum. Equation (20) becomes of the same form as Eq. (6) of Ref. 23 for homogeneous density $n_e = n_0$. Solving Eq. (20) for the fluid velocity, a reasonably good approximation is

$$v_{ex} = \frac{p_{ex}}{m_*\gamma}, \quad \gamma = \frac{1}{G}\left(1 + G^3\frac{|p_{ex}|^3}{m_*^3 v_F^3}\right)^{1/3}, \tag{22}$$

where γ takes the role of an effective semi-relativistic gamma factor, and $G = 4/(1+3n_e/n_0)$ takes into account the compression of the electron density. Figure 2 shows v_{ex} as a function of p_{ex} for different values of n_e/n_0 using Eq. (20) and the numerical fit in Eq. (22). In the small amplitude limit (with $n_e/n_0 = 1$), the linear relationship is $v_{ex} = p_{ex}/m_*$. On the other hand, in the large amplitude limit $p_{ex}v_F/\mu \gg n_e/n_0$, we have $v_{ex} = v_F\ \mathrm{sign}(p_{ex})$, consistent with the results in Refs. 23 and 24.

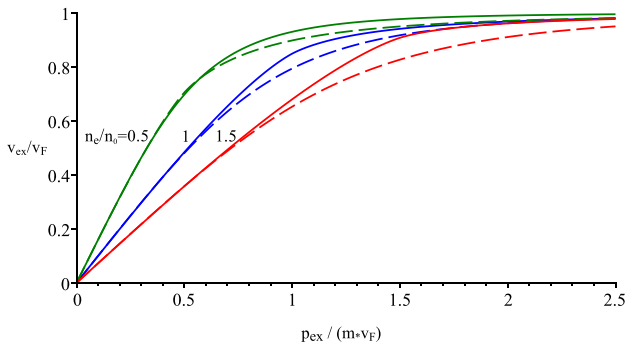

FIG. 2. The normalized fluid velocity v_{ex}/v_F as a function of the normalized fluid momentum $p_{ex}/(m_* v_F)$ for $n_e/n_0 = 0.5$, 1 and 1.5 as indicated in the figure. The solid lines show the velocity using Eq. (20) while the dashed lines show the approximation in Eq. (22).

With the distribution function given in Eq. (18), the Eq. (16) reduces to

$$\frac{\partial}{\partial t}(n_e p_{ex}) + \frac{\partial P}{\partial x} - en_e\frac{\partial\phi}{\partial x} = 0, \tag{23}$$

where the pressure $P = P_{dyn} + P_{stat}$ is expressed as the sum of the dynamic pressure mainly due to the mean flow of the electrons

$$P_{dyn} = v_F \int \frac{p_x^2}{|\mathbf{p}|} f d^2p - P_{stat}, \tag{24}$$

and the statistical pressure due to electron degeneracy

$$P_{stat} = v_F \int \frac{(p_x - p_{ex})^2}{|\mathbf{p} - \hat{\mathbf{x}}p_{ex}|} f d^2p, \tag{25}$$

with $\hat{\mathbf{x}}$ being a unit vector in the x-direction. By a change of integration variable, the fluid momentum p_{ex} is eliminated from the expression for P_{stat}. Then, introducing polar coordinates in momentum space and carrying out the integration along the radial momentum direction, we arrive at the equation of state

$$\begin{aligned} P_{stat} &= \frac{n_0\mu}{3\pi}\frac{n_e^3}{n_0^3}\int_0^{2\pi}\frac{\cos^2(\varphi)}{\sqrt{(n_e^2/n_0^2)\cos^2(\varphi) + \sin^2(\varphi)}}d\varphi \\ &\approx \frac{n_0\mu}{3\pi}\frac{n_e^3}{n_0^3}\frac{4\pi}{1+3n_e/n_0}, \end{aligned} \tag{26}$$

where, in the last step, an accurate Padé approximation was used for the integral, giving a small relative error less than 1% for $0.4 < n_e/n_0 < 4$.

To evaluate the dynamic pressure, we carry out the integral over p_x in Eq. (24) to obtain

$$P_{dyn} = \frac{n_0 v_F^3}{\pi\mu^2}\int_{p_y=-\mu/v_F}^{\mu/v_F}(s_+ - s_-)dp_y - P_{stat}, \tag{27}$$

where $s_\pm = (1/2)\left[p_{x\pm}\sqrt{p_{x\pm}^2 + p_y^2} - p_y^2 \ln\left(p_{x\pm} + \sqrt{p_{x\pm}^2 + p_y^2}\right)\right]$. An approximation of Eq. (27) is $P_{dyn} \simeq n_0 p_{ex}^2/M$, where $M = 16m_*/(9 + n_e/n_0)$ depends weakly on the compression of the electron density. The choice of compression along the x-direction was arbitrary, and in 2D, the momentum equation becomes

$$\frac{\partial(n_e\mathbf{p}_e)}{\partial t} + \nabla\cdot\left(\frac{n_0\mathbf{p}_e\mathbf{p}_e}{M}\right) + \nabla P_{stat} - en_e\nabla\phi + \nabla\psi_{kin} = 0, \tag{28}$$

with ϕ given by Eq. (4) and P_{stat} by Eq. (26). The velocity field in the continuity equation (13) is approximated as [cf. Eq. (22)]

$$\mathbf{v}_e = \frac{\mathbf{p}_e}{m_*\gamma}, \quad \gamma = \frac{1}{G}\left(1 + G^3\frac{|\mathbf{p}_e|^3}{m_*^3 v_F^3}\right)^{1/3}. \tag{29}$$

Equations (13) and (28), coupled with Eqs. (4) and (29), constitute the nonlinear fluid model. Higher order dispersive corrections based on the exact kinetic dispersion relation (8) have been taken into account by the addition of the $\nabla\psi_{kin}$ term in the left-hand side of Eq. (28), with the Fourier component of ψ_{kin} given by $\hat{\psi}_{kin} = \alpha\hat{n}_e$ and $\alpha = (\mu/8)\lambda_s k/(1+\lambda_s k/2)$. In real space, ψ is obtained via a convolution product between $(n_e - n_0)$ and the inverse Fourier transform of $\alpha(k)$; the latter can be expressed in terms of special functions but is omitted here for brevity.

To assess the validity of the model, we study the linearized system with $n_e = n_0 + n_{e1}$, $P = P_0 + P_1$, $\mathbf{p}_e = \mathbf{p}_{e1}$, $\mathbf{v}_e = \mathbf{v}_{e1}$, $\phi = \phi_1$. The linearized statistical pressure is $P_{stat,1} = (3/4)\mu n_{e1}$, while the fluid velocity and momentum are linearly related as $\mathbf{v}_{e1} = \mathbf{p}_{e1}/m_* = (v_F^2/\mu)\mathbf{p}_{e1}$. Then, assuming n_{e1}, $\mathbf{p}_{e1}$ and ϕ_1 to be proportional to $\exp(i\mathbf{k}\cdot\mathbf{r} - i\omega t)$, and using that the Fourier component $\hat{\phi}$ of the potential is related to the electron density $\hat{n}_e$ as $\hat{\phi} = -e\hat{n}_e/(2\epsilon_0\epsilon|k|)$, the Fourier components are eliminated from the linearized system. Neglecting ψ_{kin} in Eq. (28) leads to a dispersion relation identical to Eq. (9), obtained from the Vlasov-Poisson system in the long wavelength limit and previously derived using a random phase approximation.[21] The inclusion of the ψ_{kin} term yields the exact kinetic dispersion relation Eq. (8).

Using a simplified nonlinear fluid model of a 2D plasma layer[41] it was found that large-amplitude waves give rise to a non-linear frequency up-shift (similar to Stokes waves), and a modulational instability due to self-amplifying sidebands of the carrier wave. Such an investigation of the present fluid model, including the effects of the nonlinear relation (29) between $\mathbf{v}_e$, $\mathbf{p}_e$, and n_e, is planned for future research.

IV. CONCLUSIONS

We have derived a non-linear fluid model for high-frequency plasmons in graphene, by taking moments of the collision-less Boltzmann (Vlasov) equation, and finding a closure corresponding to adiabatic compression and rarefaction of the electron density in the wave-field. Higher order linear dispersive effects are added to the fluid model by using the exact linear dispersion relation obtained from semiclassical kinetic theory. We emphasize that the nonlinearity in Eq. (29) and in the second and third terms of Eq. (28) give rise to nonlinear currents that can be used for high-order harmonic generation and frequency multiplication in the response of harmonic large-amplitude electromagnetic waves,[23,24] and may lead to the localization of plasmon wave energy via modulational instabilities[41] and to wave localization and the formation of solitons.[39,40] A positive nonlinear frequency shift through self-interaction of waves was predicted in Ref. 41 for a 2D electron gas, but for graphene, the increase of the effective mass through the semi-relativistic gamma factor in Eq. (29) may lead to a *negative* frequency shift, in analogy with large-amplitude Langmuir waves[55,56] and electromagnetic waves[55,57,58] in 3D classical plasmas where the relativistic mass increase of the electrons leads to an effective decrease in the plasma frequency. Thus, a few applications of the nonlinear fluid model can be to study the nonlinear wave–wave interaction between plasmons and the nonlinear coupling and scattering between plasmons and electromagnetic waves in graphene.

ACKNOWLEDGMENTS

This work was supported by the Engineering and Physical Sciences Research Council (EPSRC), UK, Grant No. EP/M009386/1. There are no data associated with this paper.

[1]K. S. Novoselov, A. K. Geim, S. V. Morozov, D. Jiang, Y. Zhang, S. V. Dubonos, I. V. Grigorieva, and A. A. Firsov, "Electric field effect in atomically thin carbon films," Science **306**, 666–669 (2004).
[2]K. S. Novoselov, D. Jiang, F. Schedin, T. J. Booth, V. V. Khotkevich, S. V. Morozov, and A. K. Geim, "Two-dimensional atomic crystals," Proc. Natl. Acad. Sci. U.S.A. **102**, 10451–10453 (2005).
[3]K. S. Novoselov, A. K. Geim, S. V. Morozov, D. Jiang, M. I. Katsnelson, I. V. Grigorieva, S. V. Dubonos, and A. A. Firsov, "Two-dimensional gas of massless Dirac fermions in graphene," Nature **438**, 197–200 (2005).
[4]M. Müller, J. Schmalian, and L. Fritz, "Graphene: A nearly perfect fluid," Phys. Rev. Lett. **103**, 025301 (2009).
[5]S. Ulstrup, J. C. Johannsen, F. Cilento, J. A. Miwa, A. Crepaldi, M. Zacchigna, C. Cacho, R. Chapman, E. Springate, S. Mammadov, F. Fromm, C. Raidel, T. Seyller, F. Parmigiani, M. Grioni, P. D. C. King, and P. Hofmann, "Ultrafast dynamics of massive Dirac fermions in bilayer graphene," Phys. Rev. Lett. **112**, 257401 (2014).
[6]A. N. Grigorenko, M. Polini, and K. S. Novoselov, "Graphene plasmonics," Nat. Photonics **6**, 749–758 (2012).
[7]X. Luo, T. Qiu, W. Lu, and Z. Ni, "Plasmons in graphene: Recent progress and applications," Mater. Sci. Eng., R **74**, 351–376 (2013).
[8]S. H. Abedinpour, G. Vignale, A. Principi, M. Polini, W.-K. Tse, and A. H. MacDonald, "Drude weight, plasmon dispersion, and ac conductivity in doped graphene sheets," Phys. Rev. B **84**, 045429 (2011).
[9]A. Nagashima, K. Nuka, H. Itoh, T. Ichinokawa, C. Oshima, S. Otani, and Y. Ishizawa, "Two-dimensional plasmons in monolayer graphite," Solid State Commun. **83**(8), 581–585 (1992).
[10]Y. Liu, R. F. Willis, K. V. Emtsev, and T. Seyller, "Plasmon dispersion and damping in electrically isolated two-dimensional charge sheets," Phys. Rev. B **78**, 201403(R) (2008).
[11]S. Y. Shin, N. D. Kim, J. G. Kim, K. S. Kim, D. Y. Noh, K. S. Kim, and J. W. Chung, "Control of the π plasmon in a single layer graphene by charge doping," Appl. Phys. Lett. **99**, 082110 (2011).
[12]J. Lu, K. P. Loh, H. Huang, W. Chen, and A. T. S. Wee, "Plasmon dispersion on epitaxial graphene studied using high-resolution electron energy-loss spectroscopy," Phys. Rev. B **80**, 113410 (2009).
[13]B. Wunsch, T. Stauber, F. Sols, and F. Guinea, "Dynamical polarization on graphene at finite doping," New J. Phys. **8**, 318 (2006).
[14]E. H. Hwang and S. Das Sarma, "Dielectric function, screening, and plasmons in two-dimensional graphene," Phys. Rev. B **75**, 205418 (2007).
[15]M. Polini, R. Asgari, G. Borghi, Y. Barlas, T. Pereg-Barnea, and A. H. MacDonald, "Plasmons and the spectral function of graphene," Phys. Rev. B **77**, 081411(R) (2008).
[16]S. Das Sarma and E. H. Hwang, "Collective modes of the massless Dirac plasma," Phys. Rev. Lett. **102**, 206412 (2009).
[17]A. Hill, S. A. Mikhailov, and K. Ziegler, "Dielectric function and plasmons in graphene," Europhys. Lett. **87**, 27005 (2009).
[18]A. Principi, M. Polini, and G. Vignale, "Linear response of doped graphene sheets to vector potentials," Phys. Rev. B **80**, 075418 (2009).
[19]T. Tudorovskiy and S. A. Mikhailov, "Intervalley plasmons in graphene," Phys. Rev. B **82**, 073411 (2010).
[20]A. Y. Nikitin, T. Low, and L. Martin-Moreno, "Anomalous reflection phase of graphene plasmons and its influence on resonators," Phys. Rev. B **90**, 041407(R) (2014).
[21]F. Stern, "Polarizability of a two-dimensional electron gas," Phys. Rev. Lett. **18**, 546–548 (1967).
[22]C. C. Grimes and G. Adams, "Observation of two-dimensional plasmons and electron-ripplon scattering in a sheet of electrons on liquid helium," Phys. Rev. Lett. **36**(3), 145–148 (1976).
[23]S. A. Mikhailov, "Non-linear electromagnetic response of graphene," Europhys. Lett. **79**(2), 27002 (2007).

[24]S. A. Mikhailov and K. Ziegler, "Nonlinear electromagnetic response of graphene: Frequency multiplication and the self-consistent-field effects," J. Phys.: Condens. Matter **20**, 384204 (2008).
[25]J. L. Cheng, N. Vermeulen, and J. E. Sipe, "Third order optical nonlinearity of graphene," New J. Phys. **16**, 053014 (2014).
[26]J. L. Cheng, N. Vermeulen, and J. E. Sipe, "Third-order nonlinearity of graphene: Effects of phenomenological relaxation and finite temperature," Phys. Rev. B **91**, 235320 (2015); *ibid*. **93**, 039904 (2016).
[27]S. A. Mikhailov, "Quantum theory of the third-order nonlinear electrodynamic effects of graphene," Phys. Rev. B **93**, 085403 (2016).
[28]S. A. Mikhailov, "Nonperturbative quasiclassical theory of the nonlinear electrodynamic response of graphene," Phys. Rev. B **95**, 085432 (2017).
[29]J. Wang, Y. Hernandez, M. Lotya, J. N. Coleman, and W. J. Blau, "Broadband nonlinear optical response of graphene dispersions," Adv. Mater. **21**, 2430–2435 (2009).
[30]E. Hendry, P. J. Hale, J. Moger, A. K. Savchenko, and S. A. Mikhailov, "Coherent nonlinear optical response of graphene," Phys. Rev. Lett. **105**, 097401 (2010).
[31]T. Gu, N. Petrone, J. F. McMillan, A. van der Zande, M. Yu, G. Q. Lo, D. L. Kwong, J. Hone, and C. W. Wong, "Regenerative oscillation and four-wave mixing in graphene optoelectronics," Nat. Photonics **6**, 554–559 (2012).
[32]Y. Wu, B. C. Yao, Q. Y. Feng, X. L. Cao, X. Y. Zhou, Y. J. Rao, Y. Gong, W. L. Zhang, Z. G. Wang, Y. F. Chen, and K. S. Chiang, "Generation of cascaded four-wave-mixing with graphene-coated microfiber," Photonics Res. **3**(2), A64–A68 (2015).
[33]X. Yao, M. Tokman, and A. Belyanin, "Efficient nonlinear generation of THz plasmons in graphene and topological insulators," Phys. Rev. Lett. **112**, 055501 (2014).
[34]R. J. Koch, T. Seyller, and J. A. Schaefer, "Strong phonon-plasmon coupled modes in the graphene/silicon carbide heterosystem," Phys. Rev. B **82**, 201413 (2010).
[35]S. Yamashita, "A tutorial on nonlinear photonic applications of carbon nanotube and graphene," J. Lightwave Technol. **30**(4), 427–447 (2012).
[36]G. Robb, "Ultra-tunable graphene light source," Nat. Photonics **10**, 3–4 (2016).
[37]S. A. Mikhailov, "Theory of the giant plasmon-enhanced second-harmonic generation in graphene and semiconductor two-dimensional electron systems," Phys. Rev. B **84**, 045432 (2011).
[38]M. L. Nesterov, J. Bravo-Abad, A. Yu. Nikitin, F. J. García-Vidal, and L. Martin-Moreno, "Graphene supports the propagation of subwavelength optical solitons," Laser Photonics Rev. **7**, L7–L11 (2013).
[39]D. A. Smirnova, I. V. Shadrivov, I. A. Smirnov, and Y. S. Kivshar, "Dissipative plasmon-solitons in multilayer graphene," Laser Photonics Rev. **8**, 291–296 (2014).
[40]D. A. Smirnova, R. E. Noskov, L. A. Smirnov, and Y. S. Kivshar, "Dissipative plasmon solitons in graphene nanodisk arrays," Phys. Rev. B **91**, 075409 (2015).
[41]B. Eliasson and C. S. Liu, "Nonlinear plasmonics in a two-dimensional plasma layer," New J. Phys. **18**, 053007 (2016).
[42]R. Roldán, J.-N. Fuchs, and M. O. Goerbig, "Collisionless hydrodynamics of doped graphene in a magnetic field," Solid State Commun. **175–176**, 114–118 (2013).
[43]M. Akbari-Moghanjoughi, "Quantum Bohm correction to polarization spectrum of graphene," Phys. Plasmas **20**, 102115 (2013).
[44]D. Kremp, M. Schlanges, and W.-D. Kraeft, *Quantum Statistics of Nonideal Plasmas* (Springer, Berlin, 2005).
[45]P. K. Shukla and B. Eliasson, "Nonlinear collective interactions in quantum plasmas with degenerate electron fluids," Rev. Mod. Phys. **83**, 885–906 (2011).
[46]F. Haas, *Quantum Plasmas: An Hydrodynamic Approach* (Springer, Berlin, 2011).
[47]R. Balescu and W. Y. Zhang, "Kinetic equation, spin hydrodynamics and collisional depolarization rate in a spin-polarized plasma," J. Plasma Phys. **40**(2), 215–234 (1988).
[48]J. Hurst, O. Morandi, G. Manfredi, and P.-A. Hervieux, "Semiclassical Vlasov and fluid models for an electron gas with spin effects," Eur. Phys. J. D **68**, 176 (2014).
[49]S. C. Cowley, R. M. Kulsrud, and E. Valeo, "A kinetic equation for spin-polarized plasmas," Phys. Fluids **29**(2), 430–441 (1986).
[50]J. Zamanian, M. Marklund, and G. Brodin, "Scalar quantum kinetic theory for spin-1/2 particles: Mean field theory," New J. Phys. **12**, 043019 (2010).
[51]A. Putaja, E. Räsänen, R. van Leeuwen, J. G. Vilhena, and M. A. L. Marques, "Kirzhnits gradient expansion in two dimensions," Phys. Rev. B **85**, 165101 (2012).
[52]Z. A. Moldabekov, M. Bonitz, and T. S. Ramazanov, "Gradient correction and Bohm potential for two- and one-dimensional electron gases at a finite temperature," Contrib. Plasma Phys. **57**, 499–505 (2017).
[53]I. Tokatly and O. Pankratov, "Hydrodynamic theory of an electron gas," Phys. Rev. B **60**, 15550 (1999).
[54]B. Eliasson and P. K. Shukla, "Nonlinear quantum fluid equations for a finite temperature Fermi plasma," Phys. Scr. **78**, 025503 (2008).
[55]A. I. Akhiezer and R. V. Polovin, "Theory of wave motion of an electron plasma," Sov. Phys. JETP **3**(5), 696–705 (1956) [Zh. Eksp. Teor. Fiz. **30**, 915 (1956) (in Russian)]; available at http://www.jetp.ac.ru/cgi-bin/e/index/e/3/5/p696?a=list.
[56]M. N. Rosenbluth and C. S. Liu, "Excitation of plasma waves by two laser beams," Phys. Rev. Lett. **29**(11), 701–705 (1972).
[57]C. Max and F. Perkins, "Strong electromagnetic waves in overdense plasmas," Phys. Rev. Lett. **27**, 1342 (1971).
[58]P. Kaw and J. Dawson, "Relativistic nonlinear propagation of laser beams in cold overdense plasmas," Phys. Fluids **13**(2), 472–481 (1970).